

## BIOCHEMISTRY

# Cardiolipin, conformation, and respiratory complex-dependent oligomerization of the major mitochondrial ADP/ATP carrier in yeast

N. Senoo, S. Kandasamy\*, O. B. Ogunbona<sup>†</sup>, M. G. Baile<sup>‡</sup>, Y. Lu<sup>§</sup>, S. M. Claypool<sup>||</sup>

The phospholipid cardiolipin has pleiotropic structural and functional roles that are collectively essential for mitochondrial biology. Yet, the molecular details of how this lipid supports the structure and function of proteins and protein complexes are poorly understood. To address this property of cardiolipin, we use the mitochondrial adenosine 5'-diphosphate/adenosine 5'-triphosphate carrier (Aac) as a model. Here, we have determined that cardiolipin is critical for both the tertiary and quaternary assembly of the major yeast Aac isoform Aac2 as well as its conformation. Notably, these cardiolipin-provided structural roles are separable. In addition, we show that multiple copies of Aac2 engage in shared complexes that are largely dependent on the presence of assembled respiratory complexes III and IV or respiratory supercomplexes. Intriguingly, the assembly state of Aac2 is sensitive to its transport-related conformation. Together, these results expand our understanding of the numerous structural roles provided by cardiolipin for mitochondrial membrane proteins.

## INTRODUCTION

Solute carriers (SLCs), the second largest family of membrane proteins (1, 2), transport metabolites across biological membranes. Of the 46 distinct SLC subfamilies, the SLC25/mitochondrial carrier family is by far the largest (2, 3). This reflects the fact that many potentially competing anabolic and catabolic pathways are housed in either the cytosol or the mitochondrial matrix, compartments that are physically separated by the mitochondrial inner membrane (IM) in which most SLC25 members reside. The most famous metabolites that must traverse the IM are adenosine 5'-triphosphate (ATP), which is primarily synthesized in the mitochondrial matrix, and its precursor adenosine 5'-diphosphate (ADP). In the context of a proton motive force across the IM, ADP/ATP carriers (Aac) alternately transport ADP and ATP, one at a time, into the matrix or toward the cytosol, respectively (4, 5); this results in a net 1:1 exchange of ADP into and ATP out of the mitochondrial matrix. Together with the phosphate carrier, another SLC25 member, Aacs are integral components of mitochondrial energy production whose activity is required for oxidative phosphorylation (OXPHOS).

Like all members of the SLC25 family, Aac is a nuclear-encoded protein consisting of roughly 300 amino acids with three approximately 100 residue repeats (two transmembrane domains per repeat), giving the carrier threefold pseudosymmetry (4, 6). Of the three isoforms identified in yeast, Aac2 is the most abundant and only isoform required for OXPHOS (7). Conformational changes in Aac are required for ADP/ATP transport across the IM. Carboxyatractyloside (CATR) and bongkrekic acid (BKA), two specific inhibitors, lock Aac in the cytosolic state (c-state; permits ligand binding from the

intermembrane space) and the matrix state (m-state; ligand binding from the matrix), respectively. The crystal structures of CATR and BKA-bound Aac led to the identification of a translocation pathway through the six transmembrane domain-containing carrier (5, 8–10). Thus, ADP/ATP transport is executed by Aac monomers. However, this by no means necessitates that ADP/ATP transport occurs normally in physical isolation.

The oligomeric status of the Aac family has been the subject of much debate. Using a range of biochemical and biophysical approaches, the first four decades of research into this issue consistently provided evidence that Aacs function as homodimers (11–14). Motivated by the crystal structures, which consisted primarily but not exclusively of monomers (5, 8–10), the oligomeric status of yeast Aacs has been systematically revisited over the past 12 years with particular emphasis on its ability to form homodimers (5, 15–18). Collectively, these studies led to the conclusion that Aacs not only function as monomers—they actually are monomeric when embedded in the IM (5, 15–18).

However, this conclusion is incompatible with the fact that the major Aac in aerobically grown yeast, Aac2, and two human Aac isoforms interact with a range of conserved heterologous proteins including respiratory supercomplexes (RSCs), import components, other mitochondrial carriers, and additional Aac isoforms (12, 19–21). Three aspects of the reported Aac interactomes are particularly relevant to the controversy surrounding Aac's oligomeric status. First, the evolutionarily conserved Aac-RSC interaction (12, 19, 20) is notable since the composition of RSCs in yeast (complexes III and IV) and humans (complexes I, III, and IV) is different (22). Thus, while the molecular details of this interaction likely display species-specific differences, the functional benefit(s) that this association confers would appear to be evolutionarily conserved. Second, endogenously expressed, nonbait Aac isoforms are copurified with yeast Aac2 and the two human Aac isoforms tested (19, 20). Given the high intraspecies sequence homology of the different Aac isoforms, this indicates that more than one copy of this carrier may be present in Aac-containing complexes. Whether this reflects interacting Aac homodimers or, instead, multiple separate Aac monomers is unclear.

Copyright © 2020  
The Authors, some  
rights reserved;  
exclusive licensee  
American Association  
for the Advancement  
of Science. No claim to  
original U.S. Government  
Works. Distributed  
under a Creative  
Commons Attribution  
NonCommercial  
License 4.0 (CC BY-NC).

Department of Physiology, Johns Hopkins University School of Medicine, Baltimore, MD, USA.

\*Present address: Research and Development, Thermo Fisher Scientific, Bangalore, India.

†Present address: Department of Pathology and Laboratory Medicine, Emory University School of Medicine, Atlanta, GA, USA.

‡Present address: Larimar Therapeutics, Bala Cynwyd, PA, USA.

§Present address: Frontier Medicines Corporation, South San Francisco, CA, USA.

||Corresponding author. Email: sclaypo1@jhmi.edu

Third, in yeast, the entire network of Aac2 interactions is dependent on the presence of the mitochondrial-specific phospholipid cardiolipin (CL) (19). CL is made in the IM (23, 24), has two headgroups and four attached fatty acyl chains, associates with every individual OXPHOS component (5, 8, 9, 25–36), and is critical for the formation and stability of RSCs (37–39), including those reported to contain Aac2 (19). Nuclear magnetic resonance studies (25) and Aac crystal structures (5, 9) have identified three tightly associated CL molecules per monomer. While minor in relative abundance compared to monomers, Aac dimers were additionally identified in several x-ray structures (5, 8), although their physiological significance has been questioned (5, 16). A large proportion of the buried surface area between dimers is provided by CL, suggesting that Aac homodimerization, if it does occur, may depend on a CL-based greasy handshake. Last, another layer of complexity into this issue stems from molecular dynamics simulations, which demonstrate that the natural proclivity of Aacs to multimerize is reduced when model membranes lack CL (40). Thus, the relationship between CL and Aac oligomerization is likely to be more complex than CL simply acting as a glue holding proteins together.

Aac2 function is compromised in yeast devoid of CL (41). The molecular details of how CL promotes Aac2 transport activity, which could derive from its ability to promote Aac2 interactions with RSCs (19, 42), have not been established. In the current study, we show that CL supports the assembly of Aac2 at two structural levels: It is essential for the ability of Aac2 to associate with RSCs, and it also stabilizes the carrier's folded state. Since two Aac-specific inhibitors can replace CL with respect to its tertiary fold but not its quaternary assembly, these two structural roles of CL for Aac2 are distinct. In the presence of CL, Aac2 adopts the c-state conformation, whereas in its absence, the carrier exists in the m-state. Thus, Aac2 conformation is also controlled by CL. Last, we show that multiple copies of Aac2 engage in shared complexes that are largely dependent on the presence of assembled respiratory complexes III and IV or RSCs. Aac2 conformation influences its ability to associate with RSCs that contain multiple copies of Aac2. Collectively, these results provide new insights into how a single lipid can promote the assembly of membrane proteins and establish that Aac2, which is essential for OXPHOS, participates in CL-dependent assemblies that may be influenced by cellular demand for mitochondrial energy.

## RESULTS

### CL has distinct structural roles for Aac assembly and conformation

Unlike mammals, which die in utero when they are unable to produce CL (38), CL-null yeast are viable and retain limited OXPHOS activity (41, 43–45). Hence, *Saccharomyces cerevisiae*, a model system commonly used to interrogate lipid-protein interactions (46, 47), is the best available eukaryotic model to probe CL-dependent protein assemblies in vivo. Using yeast, we previously demonstrated that the major yeast Aac isoform Aac2 engages in a number of distinct interactions that are dependent on CL. The mechanistic underpinnings of how CL facilitates Aac2 assembly have yet to be resolved. Like Aac2, RSC assembly and function are dependent on CL (37, 39). Notably, the CL-dependent assembly of RSCs in yeast, whereby a complex III homodimer associates with one to two copies of complex IV, is rescued by the addition of exogenous CL to mitochondria purified from *crd1Δ* yeast (37), demonstrating the specificity

of CL in supporting the association of this macromolecular machine. Whether exogenous CL has the same capacity to rescue Aac2 assembly has not been determined. In preliminary experiments, we noted that the efficiency of extracting a range of IM proteins with digitonin varied depending on whether mitochondria contained or lacked CL and was further differentially affected by the addition of exogenous lipids (fig. S1, A and B). Specifically, IM proteins contained in mitochondria lacking CL (*crd1Δ*) were solubilized at lower concentrations of digitonin than wild type (WT). Preincubating mitochondria with phosphatidylcholine (PC) reduced the solubilization efficiency of IM proteins in both WT and *crd1Δ*-derived mitochondria; the addition of bovine CL did not significantly alter the ability of digitonin to extract IM proteins. Furthermore, while the assembly of Aac2 and RSCs was insensitive to the amount of digitonin used for membrane extraction or the inclusion of either PC or CL in WT mitochondria, their assembly was notably affected in *crd1Δ*-derived mitochondria (fig. S1C). Hence, to directly compare the effects of exogenous CL and PC on Aac2 assembly in mitochondria from each strain independent of any differences in membrane solubilization, the concentration of digitonin was optimized to normalize the extraction efficiency between WT and *crd1Δ* mitochondria and following the different treatments (fig. S1, D and E). In these conditions, preincubation of *crd1Δ* mitochondria with CL partially restored Aac2 and RSC assembly in parallel (Fig. 1A and fig. S2A). These effects were titratable and specific for CL (no rescue was observed using exogenous PC). Furthermore, Aac2 and RSC assembly was not substantially altered by the addition of exogenous CL to WT mitochondria. Thus, endogenous levels of CL are sufficient to support the complete assembly of these complexes.

The Aac-specific inhibitors CATR and BKA fix the carrier in distinct conformations that are modeled to allow substrate binding and release on opposite sides of the IM (5, 10). Previously, it was shown that the anomalous migration of affinity purified Aac3 by blue native polyacrylamide gel electrophoresis (BN-PAGE) compared to Aac3 present in mitochondrial extracts is prevented by the inclusion of CATR (18), an observation taken to reflect the ability of this inhibitor to stabilize Aac tertiary structure. Furthermore, CATR and CL were demonstrated to have an additive effect in improving the thermostability of Aac2 (48). In this context and given the importance of CL for Aac2 assembly (19), we asked whether CATR or BKA could rescue these CL-sensitive Aac2-RSC assembly defects (Fig. 1B). CATR and BKA have distinct pH-binding optimums (49, 50). Aac2 assembly was not altered when mitochondria were preincubated in the absence of these inhibitors at either pH 6.0 or 7.4 before detergent solubilization. In CL-containing mitochondria, the addition of BKA predigitonin solubilization reduced the size of the major Aac2 species detected, previously shown to reflect a monomer (18), from 140 to ~100 kDa. The 140-kDa monomeric Aac2 band was stabilized by the addition of CATR. In addition, the faint smear normally detected beneath the major 140-kDa Aac2 band, which is most likely an unfolded/partially unfolded monomer, was not detected in CATR-treated samples. These results suggest that BN-PAGE has the capacity to resolve distinct Aac2 conformations and that at rest, most Aac2 is in the c-state (Aac2 without inhibitor comigrated with Aac2 that is CATR ligated), at least in the conditions used here.

In the absence of CL, the numerous high-molecular weight Aac2-containing complexes were reduced and/or destabilized, which resulted in a broad smear from ~200 to <67 kDa (Fig. 1B).

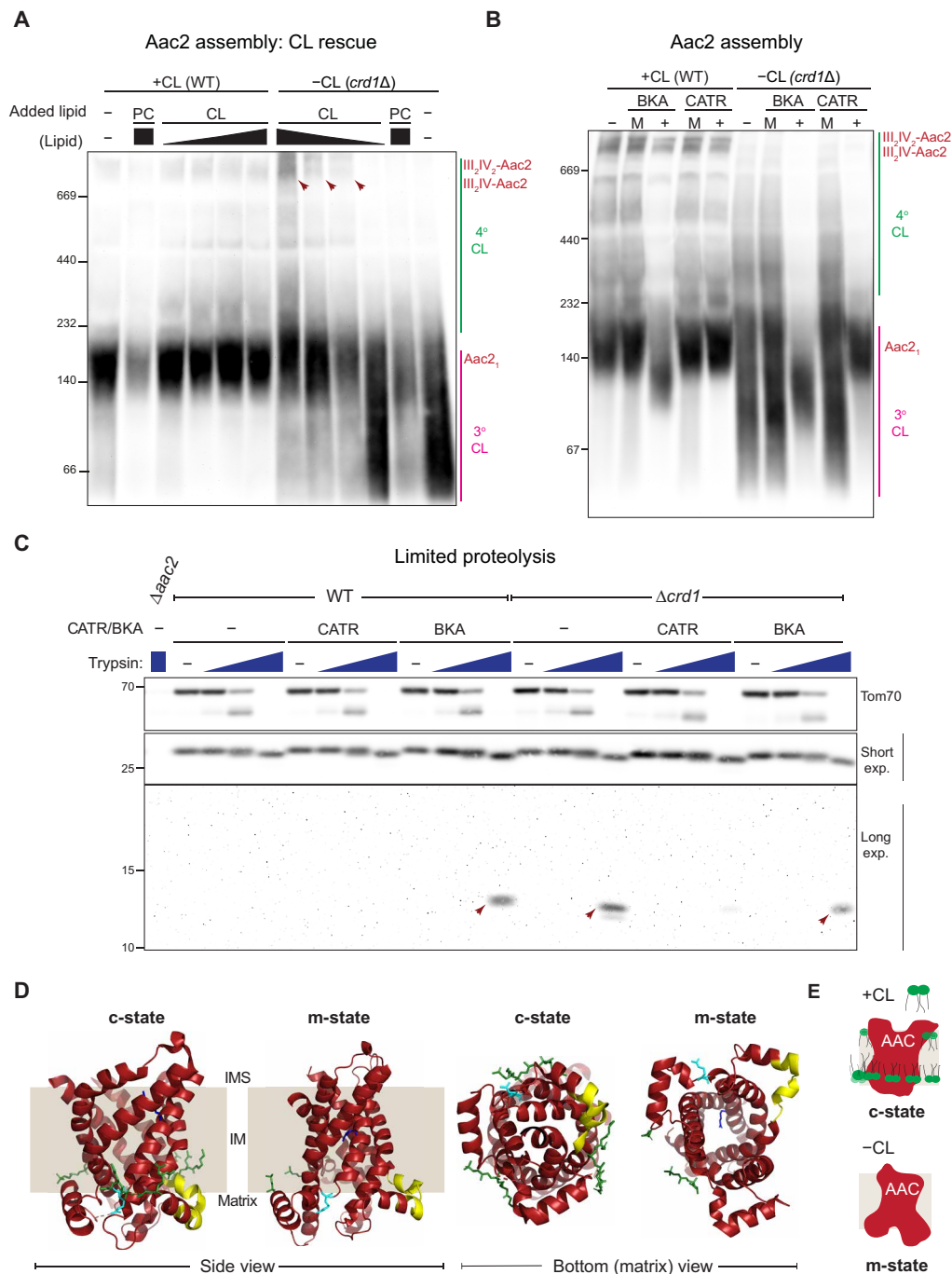


**Fig. 1. CL stabilizes the tertiary structure and quaternary assembly of Aac2 and controls its conformation.** (A) Mitochondria from WT or *crd1Δ* yeast were supplemented with PC or increasing amounts of CL (relative amount added indicated) before solubilizing them with an optimized concentration of digitonin to decrease differences in Aac2 solubilization efficiency: 1.0% (w/v) for mock (–) or CL-treated *crd1Δ* mitochondria, 1.5% (w/v) for mock (–) or CL-treated WT mitochondria and PC-treated *crd1Δ* mitochondria, and 2.0% (w/v) for PC-treated WT mitochondria. Mitochondrial extracts were resolved by 6 to 16% blue native polyacrylamide gel electrophoresis (BN-PAGE) and immunoblotted for Aac2. Red arrowheads highlight CL-restored assembly of Aac2 with RSCs. Aac2<sub>1</sub>, Aac2 monomer; III<sub>2</sub>IV<sub>2</sub>-Aac2 and III<sub>2</sub>IV-Aac2, Aac2 associated with large and small RSCs, respectively; 4° and 3°, Aac2 quaternary and tertiary assembly, respectively (n = 3). (B) WT and *crd1Δ* mitochondria (100 μg), mock-treated (M) or instead incubated with BKA (10 μM) or CATR (40 μM), were solubilized with 1.5% (w/v) digitonin, resolved by 6 to 16% BN-PAGE, and immunoblotted for Aac2 (n = 3). (C) WT and *crd1Δ* mitochondria (100 μg) were incubated with buffer, CATR (40 μM), or BKA (10 μM) and then solubilized with 1.5% (w/v) digitonin containing increasing amounts of trypsin (0, 0.5, 5, and 50 μg/ml) for 30 min on ice. After trypsin inactivation, the clarified extracts were resolved by 10 to 16% SDS-PAGE and immunoblotted as designated. For Aac2 detection, an Aac2 monoclonal antibody 2C10 was used that detects the following internal epitope (NH<sub>2</sub>-IVAAEGVGSFLFKG-COOH). (n = 3). (D) Model of the predicted trypsin site in Aac2. Aac2 in the c-state [Protein Data Bank (PDB) ID: 4C9G] or modeled in the m-state (based on PDB ID: 6GCI). The left two panels are the two conformational states (as indicated) viewed from the side, and the right two panels are the indicated conformational states viewed from the bottom (matrix facing). The 2C10 epitope is shown in yellow, CL in green, R191 in cyan, and R204 in blue. IMS, intermembrane space. (E) Schematic depicting role of CL on Aac2 conformation.

The addition of BKA or CATR rescued the predominant ~100- and 140-kDa Aac2 monomeric bands, respectively. In contrast, neither inhibitor restored the numerous high-molecular weight Aac2-containing complexes observed in CL-replete mitochondria. As expected, the assembly of complexes III and IV containing RSCs was not affected by either BKA or CATR (fig. S2B). Together, these results indicate that CL is critical for both the tertiary (pink line at the right of Aac2 immunoblot) and quaternary (green line at the right of Aac2 immunoblot) assembly of Aac2, the former of which can be substituted for by either CATR or BKA.

To our knowledge, BN-PAGE has not been previously reported capable of resolving distinct protein conformers. Therefore, as an independent means of testing Aac2 conformation in the presence and absence of CL, we performed a limited proteolysis experiment (Fig. 1C). In brief, CL-containing and CL-lacking mitochondria were incubated with nothing, CATR, or BKA and then solubilized with digitonin spiked with increasing amounts of trypsin. In mitochondria with CL, preincubation with BKA yielded a ~13-kDa proteolytic fragment that was not detected in either the untreated or CATR-exposed samples. Untreated *crd1Δ* mitochondria generated the same proteolytic fragment whose accumulation was prevented by CATR but not BKA. On the basis of the migration of the proteolytic fragment, which was detected by a monoclonal antibody recognizing a peptide in the C terminus of Aac2, and the theoretical molecular weights of Aac2 C-terminal fragments following trypsinolysis, we predict that the major cleavage site occurred between residues 185 and 205. Two potential trypsin cleavage sites (after R or K) are contained within this region: R191 and R204 (Fig. 2D). R204 (highlighted in blue) is in the middle of the fourth transmembrane domain, facing the pore in both the c- and m-states. R191 (highlighted in cyan) occurs in a loop on the matrix-facing side of Aac2. In the c-state structure, R191 is confined around the matrix helices and adjacent to CL (three CL residues detected in c-state Aac structures are highlighted in green), where it is likely protected from trypsin. Notably, in the m-state, R191 is more exposed and in a region where CL did not cocrystallize (10). Thus, this structural analysis predicts that in the absence of CATR or CL, R191 becomes accessible to trypsin and is the predominant proteolytic cleavage site in the m-state.

In our experience, BN-PAGE can be more destabilizing to proteins than alternative detergent-based assays such as coimmunoprecipitation studies (51). Therefore, we speculate that the unfolding observed for Aac2 in the absence of CL or either Aac2-specific inhibitor (Fig. 1B) reflects the additional challenges to protein structure imposed by BN-PAGE. In comparison, even though the solubilization conditions used for the limited proteolysis studies were the same as for BN-PAGE, they are likely less disruptive to protein structure. Cast in this light, the limited proteolysis results suggest that in the presence of CL, Aac2 exists primarily in the c-state, while in its absence, Aac2 adopts the m-state (Fig. 1E).

### Aac2 oligomerization is CL dependent and conformation sensitive

It has been suggested that large Aac-containing complexes detected following BN-PAGE reflect experimental limitations of this method that are linked to detergent micellar size, the presence or absence of defined lipids such as CL, and the unstable nature of Aac in detergents in the absence of folding stabilizers such as CATR, BKA, and/or CL (18, 48). Therefore, we developed a system that would allow

us to probe the ability of Aac2 to interact with other proteins, determine whether multiple copies of Aac2 participate in a shared complex(es), and assess the importance of Aac2 structural conformation and/or integrity for any interactions identified. Toward this end, hemagglutinin (HA) or FLAG tags were knocked into the N terminus of the endogenous AAC2 locus (Fig. 2, A and B). FLAG-Aac2 and HA-Aac2 both supported growth on respiratory media, although HA-Aac2 was slightly impaired relative to WT and FLAG-Aac2 (Fig. 2C). Next, haploid yeast strains with or without the ability to produce CL (*crd1Δ*) were mated to generate diploid strains that expressed varying combinations of WT Aac2, HA-Aac2, and FLAG-Aac2 at physiologically relevant levels (Fig. 2, D and E). In CL-containing mitochondria, FLAG-Aac2 and HA-Aac2 coimmunoprecipitated each other as well as representative subunits of both complex III and complex IV, to the same extent in the presence and absence of CATR (Fig. 2, F and G, and fig. S3). This indicates that in the presence of CL, Aac2 associates with itself and RSCs in a folded state whose stability is not dependent on CATR. The addition of BKA predigitonin solubilization decreased the amount of HA-Aac2 and complexes III and IV that coimmunoprecipitated with FLAG-Aac2 by 37, 25, and 50% compared to the CATR-stabilized carrier (Fig. 2, F and H).

As determined by BN-PAGE, neither CATR nor BKA was able to restore the CL-dependent assembly of Aac2 into complexes that likely represent associations with itself and/or heterologous proteins (Fig. 1B, green line at the right of Aac2 immunoblot). Consistent with this interpretation, in CL-lacking mitochondria (Fig. 3A), CATR- or BKA-stabilized FLAG-Aac2 and HA-Aac2 failed to coimmunoprecipitate each other or subunits of either complex III or complex IV (Fig. 3, B and C, and fig. S4). The combined results from the BN-PAGE (Fig. 1) and coimmunoprecipitation experiments (Figs. 2 and 3) indicate that CL promotes the tertiary and quaternary assembly of Aac2 via distinct mechanisms.

Unlike digitonin, dodecyl- $\beta$ -D-maltoside (DDM) can dissociate RSCs into their individual complexes (22). To determine the impact of DDM on Aac2, we solubilized CL-containing mitochondria with digitonin or increasing amounts of DDM and assessed Aac2 assembly by either BN-PAGE (Fig. 4A) or coimmunoprecipitation (Fig. 4B) analyses. DDM substantially altered Aac2 assembly as determined by BN-PAGE, even when used at a concentration that did not separate complexes III and IV (Fig. 4A). Adding CATR, but not BKA, before detergent extraction prevented the accumulation of the smallest Aac2 band (<67 kDa), which is interpreted as an unfolded monomer. The migration of CATR-stabilized Aac2 was notably different at low versus high DDM, which could reflect the amount of annular lipids retained in the detergent micelles in each condition. When solubilized by DDM, FLAG-Aac2 failed to coimmunoprecipitate HA-Aac2 or subunits of either complex III or complex IV regardless of whether the Aac2 tertiary fold was stabilized with CATR (Fig. 4B). These results indicate that DDM destabilizes both the CL-dependent tertiary and quaternary assembly of Aac2. Moreover, they demonstrate that the ability of Aac2 to engage in macromolecular assemblies with itself and other proteins is not a by-product of non-specific interactions that occur secondary to the exposure of its hydrophobic elements that result from its complete or partial unfolding.

### Aac2 multimerization is RSC dependent

While FLAG-Aac2 and HA-Aac2 were reciprocally coimmunoprecipitated from CL-containing mitochondria, it is unclear whether



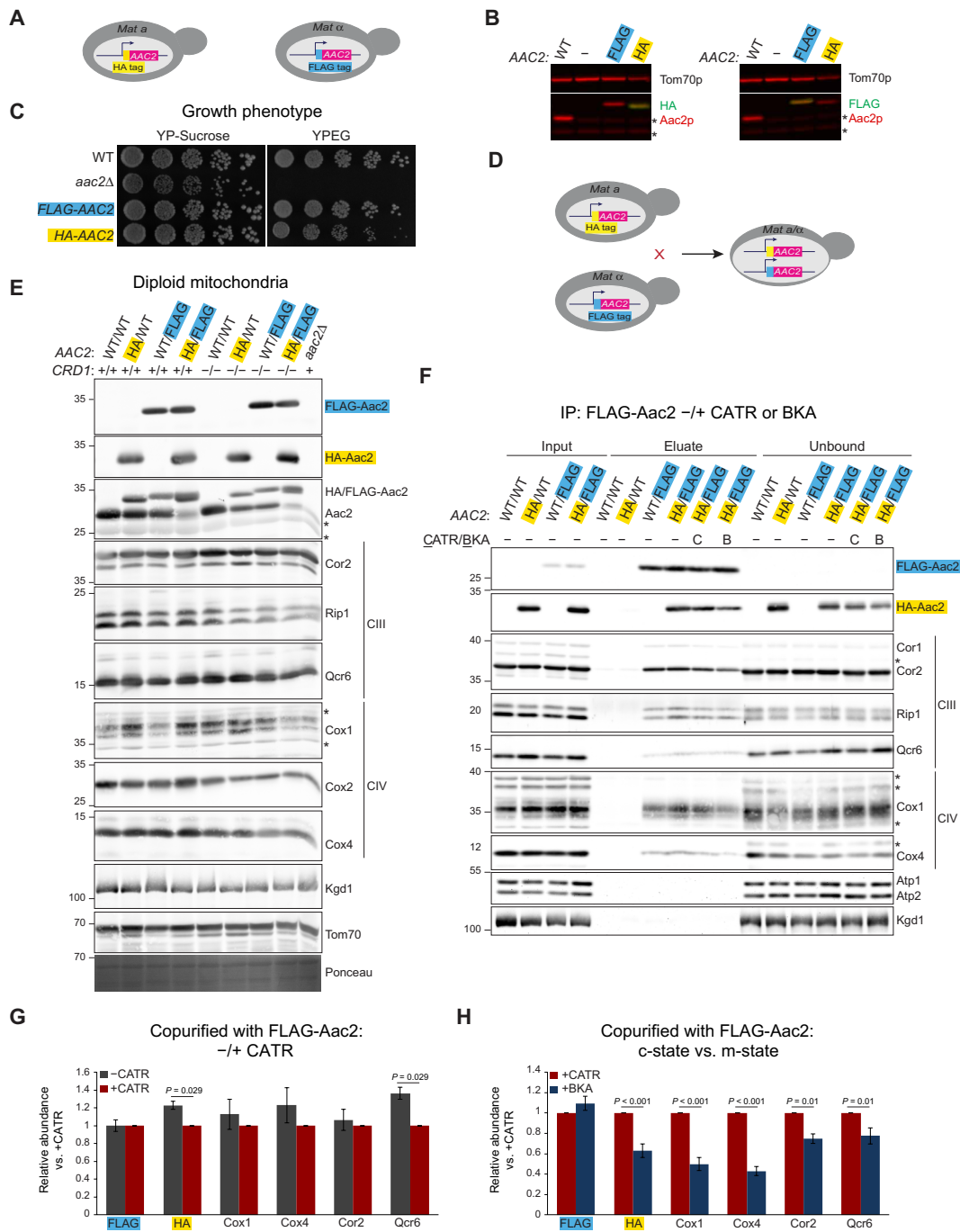


**Fig. 2. Aac2 oligomerization is conformation sensitive.** (A) Schematic representation of yeast strains expressing endogenously tagged Aac2. (B) Fluorescent immunoblots of whole-cell extracts from indicated haploid yeast strains for Aac2 (red) and either the HA or FLAG epitopes (green); Tom70 served as loading control. \*, non-specific bands ( $n = 3$ ). (C) Serial dilutions of haploid cells from indicated strains were spotted onto YP medium supplemented with sucrose YP-Sucrose or ethanol-glycerol (YPEG) and incubated at 30°C for 3 days ( $n = 3$ ). (D) Mating strategy to establish diploid yeast expressing two different endogenously tagged forms of Aac2. (E) Diploid mitochondria (20  $\mu\text{g}$ ) were resolved by 10 to 16% SDS-PAGE and immunoblotted as indicated. The migration of epitope-tagged and WT Aac2, which were codetected with an Aac2 polyclonal antisera, is indicated. \*, nonspecific bands. Bottom panel shows Ponceau S-stained membrane ( $n = 3$ ). (F) Mitochondria (250  $\mu\text{g}$ ) from the indicated CL-producing strains, preincubated with CATR (40  $\mu\text{M}$ ) or BKA (10  $\mu\text{M}$ ) as listed, were solubilized with 1.5% (w/v) digitonin and FLAG-Aac2 immunoprecipitated (IP) using anti-FLAG resin. The presence of copurified HA-Aac2 and subunits of complexes III (Cor1, Cor2, Rip1, and Qcr6) and IV (Cox1 and Cox4) was determined by immunoblotting; Atp1, Atp2, and Kgd1 served as controls. \*, nonspecific bands. Four percent of input (mitochondria) and unbound (flow through following FLAG immunoprecipitation) was analyzed ( $n = 4$ ). (G) The amount of HA-Aac2 and respiratory complex subunits coimmunoprecipitated with FLAG-Aac2 in untreated mitochondria was determined relative to mitochondria preincubated with CATR (means  $\pm$  SEM for  $n = 4$  independent experiments). (H) The amount of HA-Aac2 and respiratory complex subunits coimmunoprecipitated with FLAG-Aac2 in BKA pretreated mitochondria was determined relative to mitochondria preincubated with CATR (means  $\pm$  SEM for  $n = 8$  independent experiments). Statistical differences for (G) and (H) were determined by Mann-Whitney rank sum test.

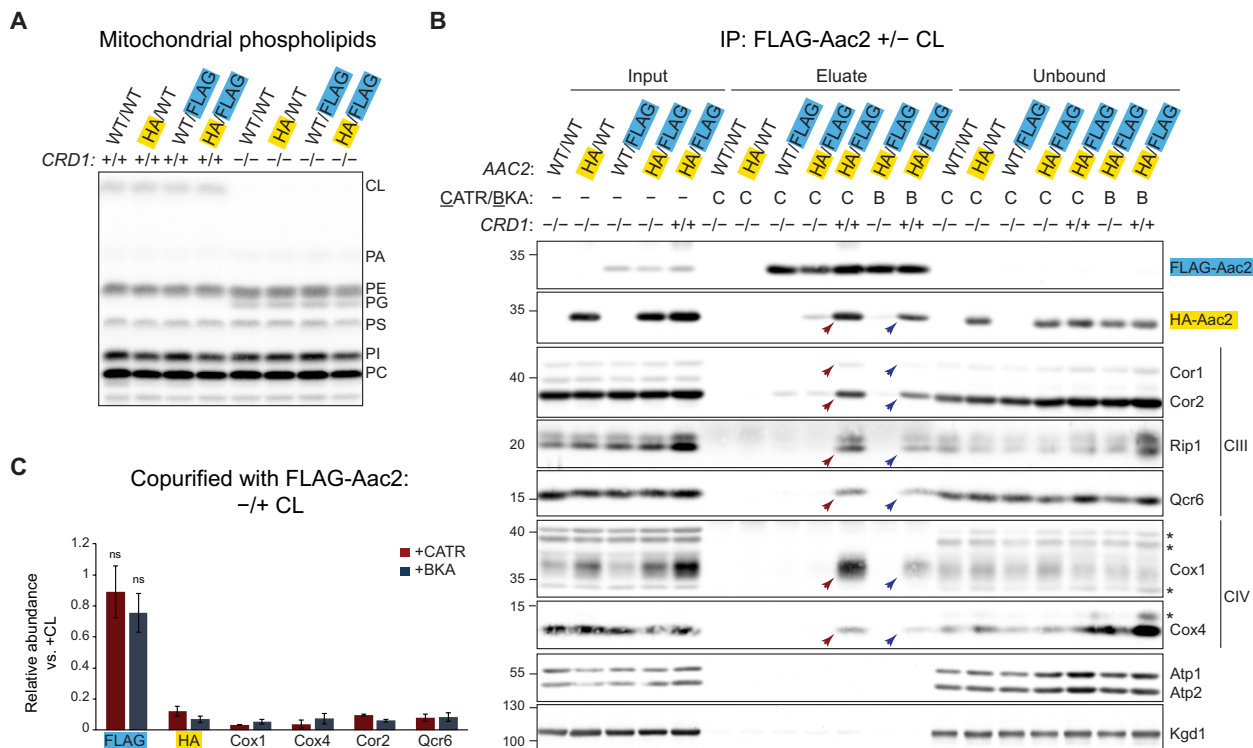


**Fig. 3. CL-dependent Aac2 oligomerization cannot be rescued with protein-stabilizing Aac2 inhibitors.** (A) Yeast strains were grown in YP-Sucrose medium supplemented with  $^{32}\text{P}$  (2.5  $\mu\text{Ci}/\text{ml}$ ) overnight. Phospholipids were extracted and separated by thin-layer chromatography (TLC). The migration of PC, phosphatidylinositol (PI), phosphatidylserine (PS), phosphatidylglycerol (PG), phosphatidylethanolamine (PE), phosphatidic acid (PA), and CL is indicated ( $n=6$ ). (B) WT or *crd1* $\Delta$  mitochondria (250  $\mu\text{g}$ ), preincubated with CATR (40  $\mu\text{M}$ ) or BKA (10  $\mu\text{M}$ ) as listed, were solubilized with 1.5% (w/v) digitonin and FLAG-Aac2 immunoprecipitated using anti-FLAG resin. The presence of copurified HA-Aac2 and subunits of complexes III (Cor1, Cor2, Rip1, and Qcr6) and IV (Cox1 and Cox4) was determined by immunoblotting; Atp1, Atp2, and Kgd1 served as controls. \*, nonspecific bands. Proteins that copurified with FLAG-Aac2 when CL-containing mitochondria were preincubated with CATR (red arrowheads) or BKA (blue arrowheads) are marked. Four percent of input (mitochondria) and unbound (flow through following FLAG immunoprecipitation) was analyzed ( $n=4$ ). (C) The amount of HA-Aac2 and respiratory complex subunits coprecipitated with FLAG-Aac2 in BKA or CATR pretreated CL-null mitochondria was determined relative to similarly treated CL-containing mitochondria (means  $\pm$  SEM for  $n=4$  independent experiments). Statistical differences were determined by Mann-Whitney rank sum test.

this reflects a direct interaction or, instead, the presence of multiple copies of Aac2 in a multiprotein complex. Given that the Aac-RSC interaction is evolutionarily conserved (19, 20), we asked whether RSCs are required for Aac2 homomultimerization. Yeast devoid of mitochondrial DNA (mtDNA) are unable to assemble respiratory complexes III, IV, and V and therefore lack RSCs. As expected, high-molecular weight Aac2-containing complexes, which include Aac2-RSC, were not detected in mitochondria isolated from yeast lacking mtDNA (Fig. 5A). Consistent with a previous report (52), mitochondrial CL levels were reduced by  $\sim 45\%$  in mitochondria from yeast lacking mtDNA compared to their mtDNA-containing parents (Fig. 5, B and C). Since the tertiary assembly of Aac2 (evidenced by smear beneath the major 140-kDa Aac2 monomeric band) was similar or improved in the absence of mtDNA, we conclude that the remaining CL levels are sufficient to support Aac2 assembly (Fig. 5A).

Next, we compared the ability of HA-Aac2 to be coimmunoprecipitated with FLAG-Aac2 in the presence or absence of RSCs. For reasons that are presently unknown, the steady-state amount of FLAG-Aac2 and HA-Aac2 was  $\sim 15$ -fold reduced in mitochondria devoid of mtDNA (Fig. 5, D and E). Hence, FLAG-Aac2 was immunoprecipitated from different quantities of mitochondria that nonetheless contained equivalent amounts of Aac2 (WT, HA-Aac2,

and/or FLAG-Aac2; *aac2* $\Delta$  mitochondria were used to normalize the total amount of protein included in each sample). Notably, the amount of HA-Aac2 copurified with FLAG-Aac2 was reduced by 90% in the absence of mtDNA (Fig. 5, F and G). This finding suggests that RSCs may contain multiple Aac2-binding sites.

### Multiple copies of Aac2 can associate with complexes III and IV

The RSC in *S. cerevisiae*, which lacks complex I, consists of a complex III homodimer attached to one to two complex IVs (22). To determine whether Aac2 associates with complex III, complex IV, or both complexes, we generated yeast strains that lacked individual subunits that are essential for the assembly of each holoenzyme (53). In mitochondria lacking Cox4 (*cox4* $\Delta$ ), a subunit of complex IV, complex III assembles but complex IV does not (Fig. 6A). Conversely, in mitochondria lacking Cor1 (*cor1* $\Delta$ ), a subunit of complex III, complex IV assembles but complex III does not. Aac2 partially comigrated with the complex III dimer in the absence of complex IV (Fig. 6A, red arrowheads) and free complex IV in the absence of complex III (Fig. 6A, blue arrowheads), suggesting that Aac2 can interact with both complexes. In both cases, the putative Aac2-containing complexes were of slightly larger size than the bulk of free complex IV or III dimer detected. CL levels were modestly reduced

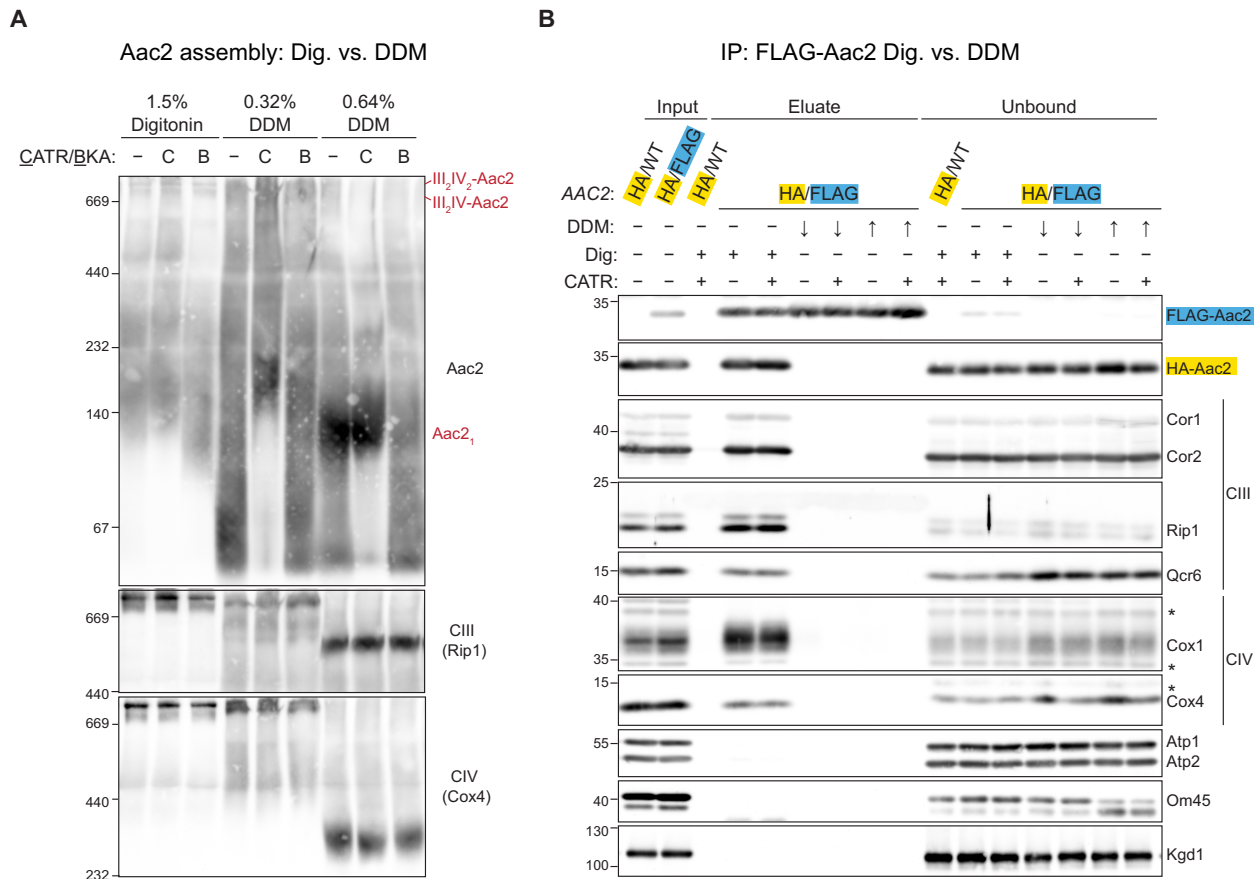


**Fig. 4. Aac2 oligomerization is specific.** (A) WT mitochondria (100  $\mu$ g), untreated (–) or instead incubated with CATR (40  $\mu$ M) or BKA (10  $\mu$ M), were solubilized with digitonin [1.5% (w/v)] or increasing amounts of DDM [0.32 and 0.64% (w/v)], resolved by 6 to 16% BN-PAGE, and immunoblotted for Aac2 (top), complex III (Rip1, middle), or complex IV (Cox4, bottom). Aac2<sub>1</sub>, Aac2 monomer; III<sub>2</sub>IV<sub>2</sub>-Aac2 and III<sub>2</sub>IV-Aac2, Aac2 associated with large and small RSCs, respectively ( $n = 4$ ). (B) WT mitochondria (250  $\mu$ g), preincubated with CATR (40  $\mu$ M) as listed, were solubilized with digitonin [1.5% (w/v)] or increasing amounts of DDM [ $\downarrow = 0.32\%$  and  $\uparrow = 0.64\%$  (w/v)], and FLAG-Aac2 immunoprecipitated using anti-FLAG resin. The presence of copurified HA-Aac2 and subunits of complexes III (Cor1, Cor2, Rip1, and Qcr6) and IV (Cox1 and Cox4) was determined by immunoblotting; Atp1, Atp2, Om45, and Kgdl served as controls. \*, nonspecific bands. Four percent of input (mitochondria) and unbound (flow through following FLAG immunoprecipitation) was analyzed ( $n = 3$ ).

in the absence of either complex III or complex IV (Fig. 6, B and C). Next, we constructed diploid strains that coexpressed either WT Aac2 and HA-Aac2 or FLAG-Aac2 and HA-Aac2, in the presence or absence of assembled complex III or IV (Fig. 6D). As suggested by BN-PAGE (Fig. 6A), FLAG-Aac2 copurified complex III subunits when complex IV was missing and complex IV subunits when complex III was absent (Fig. 6E). Intriguingly, HA-Aac2 was copurified with FLAG-Aac2 in the absence of either complex III or complex IV. Collectively, these results indicate that Aac2 engages in distinct interactions with subunits of complexes III and IV and that RSCs have the capacity to interact with multiple molecules of Aac2.

## DISCUSSION

We previously demonstrated that Aac2 physically associates with RSCs and other mitochondrial carriers, but only in the context of membranes that contain CL (19). However, these prior studies were performed in the absence of agents known to stabilize the carrier's folded state. Thus, it was formally possible, and indeed suggested (18), that the identified interactions were nonspecific in nature and

simply a consequence of Aac2 denaturation in detergent extracts. Given this limitation of our earlier study combined with the significant controversy surrounding the proposition that mitochondrial Aacs engage in interactions with itself and/or heterologous proteins, in the current study, we have revisited this issue using genetic models that avoid potential overexpression artifacts, a combination of biochemical approaches, and protein stabilizing pharmacologic tools. Our results establish that the ability of Aac2 to associate with RSCs is dependent on both the integrity of its folded state and the presence of CL. Moreover, our study has uncovered two additional structural roles provided by CL for this essential OXPHOS component: (i) CL stabilizes the native Aac2 folded state, and (ii) CL controls the preferred conformation of Aac2 in the membrane (Fig. 6F). Each of these structural properties of CL could contribute to the diminished activity of Aac2 in mitochondria devoid of CL (41), as discussed next.

While protein thermostability assays (48) and our BN-PAGE analyses (Fig. 1B) establish that CL stabilizes the tertiary structure of Aac2 when extracted with detergents, it is also evident that Aac2 is more or less properly folded in mitochondrial membranes lacking

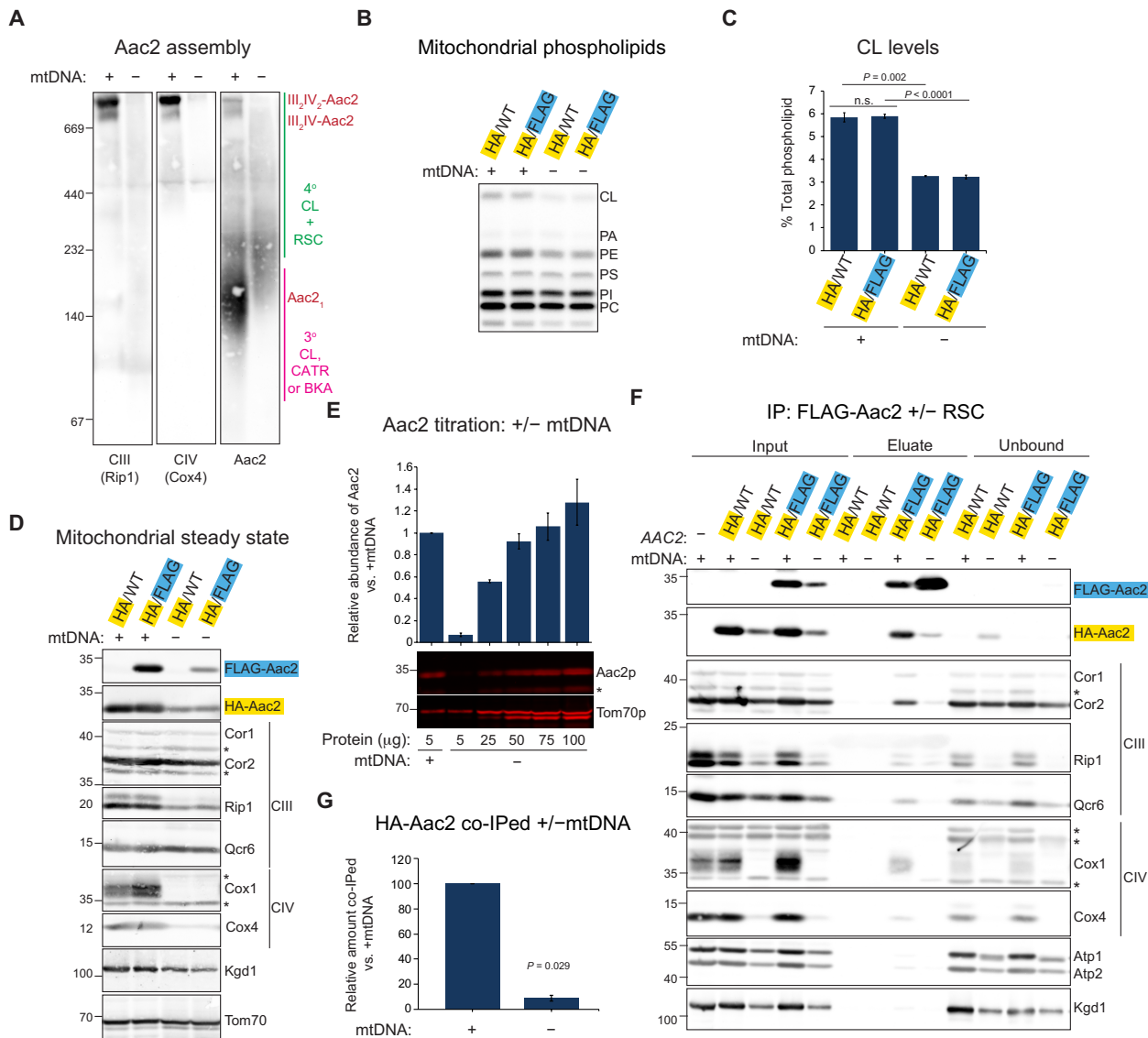


**Fig. 5. RSCs are required for Aac2 multimerization.** (A) WT (+mtDNA) and *rho-* (-mtDNA) mitochondria were solubilized with digitonin, resolved by BN-PAGE, and immunoblotted for complex III, complex IV, or Aac2. Aac2<sub>1</sub>, Aac2 monomer; III<sub>2</sub>IV<sub>2</sub>-Aac2 and III<sub>2</sub>IV-Aac2, Aac2 associated with large and small RSCs, respectively; 4° and 3°, Aac2 quaternary and tertiary assembly, respectively (*n* = 3). (B) Mitochondrial phospholipids separated by TLC and revealed by phosphorimaging. (C) The relative abundance of CL (means ± SEM for *n* = 6). Significant differences were determined by Student's *t* test (HA/FLAG + mtDNA versus HA/FLAG-mtDNA) or Mann-Whitney rank sum test (HA/WT + mtDNA versus HA/WT-mtDNA). n.s., not significant. (D) Immunoblots of diploid mitochondria. \*, nonspecific bands (*n* = 4). (E) Aac2 level as a function of mtDNA was determined (means ± SEM for *n* = 4). (F) The indicated diploid mitochondria were preincubated with CATR, solubilized with digitonin, and FLAG-Aac2 immunoprecipitated. Different quantities of mitochondria that nonetheless contained equivalent amounts of Aac2 (WT, HA-Aac2, and/or FLAG-Aac2; *aac2Δ* mitochondria were used to normalize the total amount of protein included in each sample) were used for these immunoprecipitations. The presence of copurified HA-Aac2 and subunits of complexes III and IV was determined; Atp1, Atp2, and Kgd1 served as controls. \*, nonspecific bands. Four percent of input (mitochondria) and unbound (flow through following FLAG immunoprecipitation) was analyzed (*n* = 4). (G) The amount of HA-Aac2 coimmunoprecipitated with FLAG-Aac2 without mtDNA was determined relative to mtDNA-containing mitochondria (means ± SEM for *n* = 4 independent experiments). The statistical difference was determined by Mann-Whitney rank sum test.

this lipid. This conclusion is based on the ability of protein stabilizing Aac2 inhibitors, when applied to intact CL-lacking mitochondria before detergent extraction, to prevent Aac2 unfolding upon addition of even the mild detergent digitonin. How then does the protein stabilizing activity of CL identified in detergents potentially affect Aac2 function? One possibility is that the extra stability conferred by CL is critical for the proper presentation of binding motifs required for the Aac2-RSC interactions. However, when using these

inhibitors, we noted that the ability of CL to promote the tertiary and quaternary assembly of Aac2 are separable attributes, indicating that they most likely reflect distinct CL-Aac2 interactions. Another possibility, given that ADP/ATP transport involves significant conformational changes (10), is that the improved stability provided by CL facilitates transport-related conformational transitions and/or prevents the production of abortive, dead-end conformations that may otherwise occur in its absence.



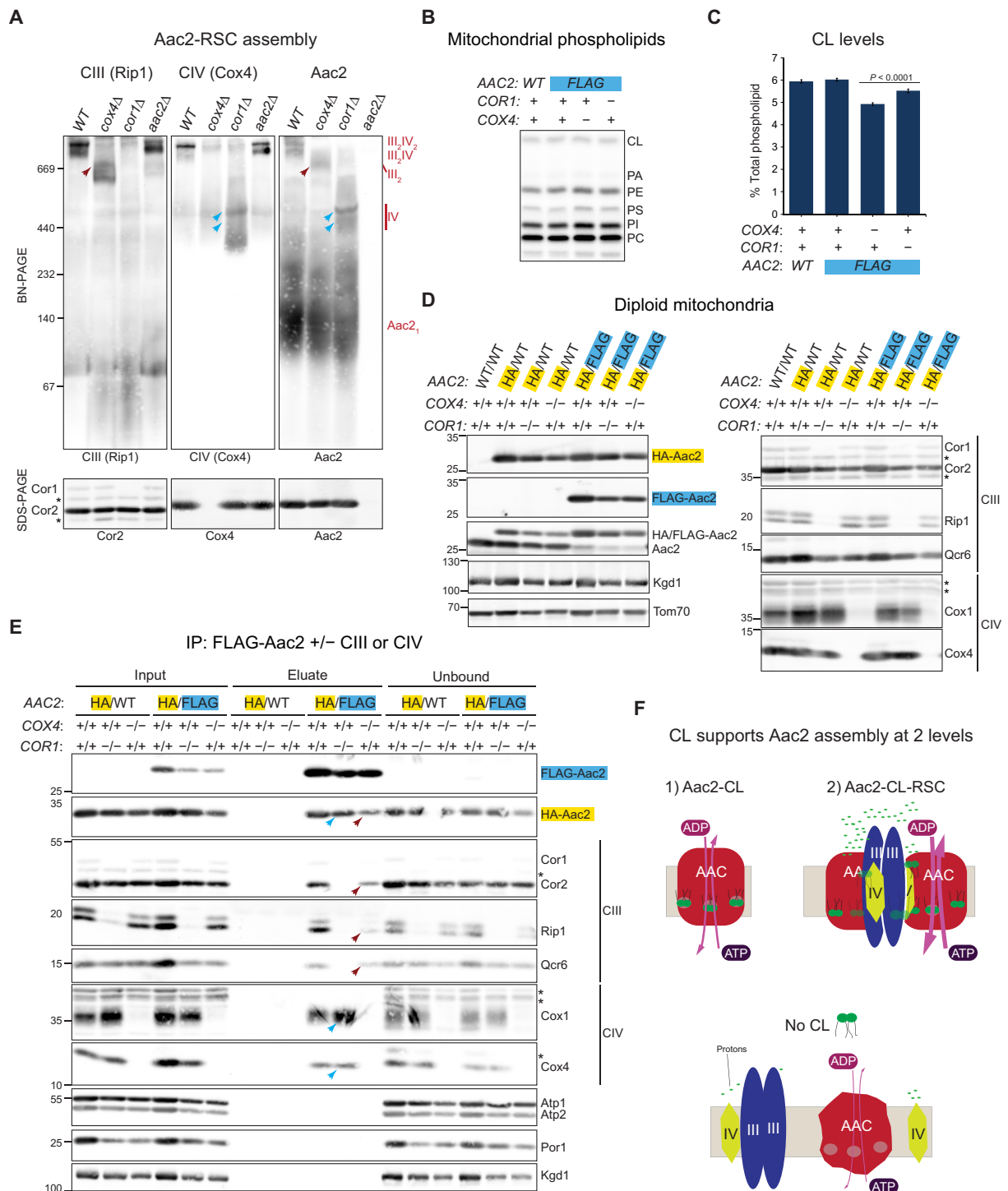


**Fig. 6. Multiple copies of Aac2 independently associate with complexes III and IV.** (A) Mitochondria from the indicated haploid strains were resolved by BN-PAGE (top three panels) to assess complex assembly and SDS-PAGE (bottom three panels) to confirm genotype. Aac2-containing complexes that comigrate with complex III in the absence of assembled complex IV (red arrowheads) or with complex IV in the absence of complex III (blue arrowheads) are highlighted. Aac2<sub>1</sub>, Aac2 monomer ( $n = 3$ ). (B) Mitochondrial phospholipids separated by TLC and revealed by phosphorimaging. (C) The relative abundance of CL (means  $\pm$  SEM for  $n = 6$ ). Significant differences relative to WT were determined by one-way analysis of variance (ANOVA) with Holm-Sidak pairwise comparisons. (D) Immunoblots of diploid mitochondria. \*, nonspecific bands ( $n = 3$ ). (E) The indicated diploid mitochondria were preincubated with CATR, solubilized with digitonin, and FLAG-Aac2 immunoprecipitated. The presence of copurified HA-Aac2 and subunits of complexes III and IV was determined; Atp1, Atp2, Por1, and Kgd1 served as controls. Four percent of input (mitochondria) and unbound (flow through following FLAG immunoprecipitation) was analyzed ( $n = 3$ ). (F) Cartoons depicting the two structural levels supported by CL for Aac2 assembly. In membranes that contain CL, CL stabilizes the Aac2 tertiary fold and is essential for the interaction of Aac2 with RSCs (note that Aac2 and RSCs are not drawn to scale). In the absence of CL, the tertiary and quaternary assembly of Aac2, as well as its activity, is compromised.

We determined that CL controls the preferred conformation of Aac2 in the IM (Fig. 1C). The central translocation pore of Aac is alternately guarded by salt bridge networks on either its cytoplasmic or matrix side that are sequentially made and broken with each transport event (5, 10, 54). In the *c*-state, the salt bridge network is intact on the matrix side but broken on the intermembrane space side. Upon binding ADP from the intermembrane space, Aac undergoes molecular rearrangements that break and establish the salt bridge networks on the matrix and intermembrane space side of the translocation pore, respectively, thus transitioning Aac into the *m*-state. Upon release of ADP into the matrix and binding ATP, Aac cycles back to the *c*-state. Unexpectedly, we show here that BN-PAGE has the capacity to resolve these two distinct transport-related Aac2 conformers (Fig. 1B). To independently confirm that BN-PAGE has this capability, we performed a limited proteolysis experiment. Results from this analysis provide compelling evidence that in CL-containing membranes, the vast majority of Aac2 is in the *c*-state, while in its absence, it is mostly in the *m*-state. While the molecular basis underpinning this observation is not known, we can envision at least two possibilities. First, in the absence of CL, OXPHOS efficiency is notably impaired (19, 41, 43–45). Thus, it is likely that the energy charge in the form of the ATP:ADP ratio is reduced in CL-lacking yeast. Changes in the ATP:ADP ratio in the cytosol and/or matrix or alterations in the preferred transport direction could, in principle, secondarily affect the steady-state conformation of Aac2. The second possibility is that perhaps CL contributes to the relative strength of either the intermembrane space–juxtaposed or matrix-facing salt bridge network. If these alterations were unevenly distributed, then they could affect the predisposition of Aac2 to adopt a given conformation and likely impede the normal operation of the carrier.

The CL-dependent association of Aac2 with RSCs, which is specific as it does not occur in conditions that disrupt both its tertiary and quaternary assembly (Fig. 4), could augment Aac2 transport while benefitting RSC activity. Specifically, the electrogenic exchange of  $\text{ADP}_{\text{in}}/\text{ATP}_{\text{out}}$  by Aac is positively influenced by the membrane potential ( $\Delta\Psi$ ) across the IM (55), which, of course, is established by the electron transport chain. Similarly, by dissipating the electrical gradient, productive Aac transport makes it easier for RSCs to pump protons. Hence, we hypothesize that this known functional synergy is further enhanced by being physically associated. Our demonstration that multiple copies of Aac2 can bind separately to complexes III and IV offers the possibility that RSCs can accommodate four or more Aac2 molecules, depending on the stoichiometry of the RSC ( $\text{III}_2\text{IV}$  or  $\text{III}_2\text{IV}_2$ ) and whether RSC formation preserves or masks a binding site. Such an arrangement would amplify the postulated functional synergy of the Aac2-RSC interaction.

Alternatively, the conserved CL-dependent Aac-RSC association may have evolved as a by-product of the environment in which they must function: the extremely protein-dense IM. In addition to having an unusually high protein:lipid ratio, another defining feature of the IM is that it is the primary membrane compartment containing CL. While the recent slew of RSC structures has firmly established that they are real entities (56–59), how they benefit mitochondria is yet unresolved. One intriguing hypothesis recently put forth is that RSCs preserve OXPHOS function in the context of the protein-dense IM (60). By extension, it is reasonable to speculate that the CL-dependent Aac-RSC interaction may protect mitochondrial fitness by a similar basic principle. In this regard, CL may serve as a molecular

bumper that, in the context of an inner mitochondrial membrane protein traffic jam, promotes mitochondrial function by preventing potentially destructive molecular interactions from occurring. In principle, the protein-stabilizing activity of CL for Aac2 could also help the carrier function in this crowded membrane environment. Defining exactly how the CL-dependent Aac-RSC interaction supports mitochondrial function will provide a more comprehensive understanding of mitochondrial bioenergetics by establishing the rationale for the higher-order assembly of its numerous proteins and protein complexes. In turn, such information will provide novel insight into mitochondrial disease, including the numerous human pathologies associated with disturbances in CL metabolism (24, 61, 62).

An important point to make explicit is that in the conditions used in this study, which is following solubilization with digitonin, most of the Aac2 is monomeric and the Aac2-RSC ensemble is clearly substoichiometric. Because this is an inherent limitation of our approach in using detergent to define and measure Aac2 interactions, it is possible that we are underestimating the Aac2-RSC association. Another limitation of our work is its use of the protein-stabilizing Aac inhibitors CATR and BKA. By systematically comparing key elements and domains of the CATR- and BKA-bound Aac, it was recently demonstrated that each inhibitor induces slight structural changes that lock the carrier in distinct, inhibitor-specific, inactive states (10). Since the amount of Aac2, complex III, and complex IV that coimmunoprecipitated with FLAG-Aac2 was similar in the absence and presence of CATR (Fig. 2G), we conclude that the minor structural changes that occur upon CATR binding do not affect the quaternary assembly of Aac2. In contrast, the molecular basis for the reduced association of Aac2 with RSCs when it is ligated to BKA is less clear. One possibility is that this is simply an artifact of the structural changes induced upon binding BKA. The more interesting alternative possibility is that indeed, the ability of Aac2 to participate in macromolecular assemblies is influenced by its transport-related conformation. If true, then it will be intriguing to contemplate how this property could be exploited to affect Aac2 interactions in a dynamic and potentially metabolically sensitive manner.

The multifaceted manner in which CL promotes Aac assembly as defined in the current study suggests numerous potential mechanisms by which this single lipid can affect ADP/ATP transport that can be experimentally tested. Three evolutionarily conserved CL-binding pockets have been identified in every available Aac structure solved thus far. Thus, mutant Aac2 constructs engineered to prevent CL binding at each pocket can be used to test whether their occupancy with CL is responsible for its protein-stabilizing and/or conformation-determining effects on Aac2. One approach to experimentally interrogate the hypothesized functional benefits provided by an Aac-RSC assembly would be to establish a series of Aac2 alleles that are defective in specific interactions with either complex III or complex IV even in the presence of CL. These interaction-null Aac2 constructs could then be leveraged to determine whether and how the Aac2-RSC association promotes optimal OXPHOS. This could be done in CL-containing mitochondria, thereby circumventing the multitude of mitochondrial functions that are compromised when this lipid is absent.

## MATERIALS AND METHODS

### Experimental design

The objective of this study was to conclusively resolve the controversy surrounding Aac oligomerization. To do so, we developed a

series of reagents and approaches that allowed us to systematically address the many ways in which CL supports Aac assembly and conformation. In addition, we used genetic models that coexpressed Aac molecules harboring different epitope tags at physiologic levels and biochemical approaches to ascertain additional Aac oligomerization requirements.

### Yeast strains and growth conditions

All yeast strains used were derived from *S. cerevisiae* parental strain GA74-1A (*MAT $\alpha$* , *his3-11,15*, *leu2*, *ura3*, *trp1*, *ade8*, *rho*<sup>+</sup>, and *mit*<sup>+</sup>) or GA74-6A (*MAT $\alpha$* , *his3-11,15*, *leu2*, *ura3*, *trp1*, *ade8*, *rho*<sup>+</sup>, and *mit*<sup>+</sup>). *aac2 $\Delta$*  and *aac2 $\Delta$ crd1 $\Delta$*  were generated by replacing the entire open reading frame of *AAC2* and *CRD1* with markers *HIS3MX6* and *TRP1*, as previously described (19) via polymerase chain reaction (PCR)-mediated gene replacement (63). For FLAG- and HA-tagged Aac2, *aac2 $\Delta$*  strains of opposite mating type were generated by replacing the entire open reading frame of *AAC2* with *URA3MX*. Each tag sequence (FLAG tag-DYKDDDDK and HA tag-YPYDVPDYA) was added onto the N terminus of the *AAC2* open reading frame by overlap extension PCR and cloned into pRS315. Following PCR amplification of the HA- or FLAG-tagged construct, *aac2 $\Delta$*  (*URA3MX*-based) yeast were transformed. Homologous recombinants were selected for by growth in rich dextrose medium containing 0.1% (w/v) 5-fluoroorotic acid and positive clones identified by immunoblotting for the appropriate epitope tag. *cor1 $\Delta$*  and *cox4 $\Delta$*  yeast were generated by replacing the open reading frame of *COR1* and *COX4*, respectively, with *HIS3MX6* or *TRP1*. Clones were selected on synthetic dropout medium [0.17% (w/v) yeast nitrogen base, 0.5% (w/v) ammonium sulfate, 0.2% (w/v) dropout mix synthetic-his or trp, and 2% (w/v) dextrose] and verified by immunoblot. To generate diploids, strains from GA74-1A and GA74-6A background were transformed with pRS315 and pRS316, respectively, and mated for 3 hours in rich dextrose media containing sterile filtered adenine (0.02 mg/ml). Resulting diploid strains were selected on synthetic dropout media [0.17% (w/v) yeast nitrogen base, 0.5% (w/v) ammonium sulfate, 0.2% (w/v) dropout mix complete, histidine (20 mg/liter), tryptophan (20 mg/liter), and 2% (w/v) dextrose]. mtDNA depleted strains were generated as described previously (64). Yeast were grown in nutrient-rich YP [1% (w/v) yeast extract and 2% (w/v) tryptone] media that contained 2% (w/v) dextrose (Fig. 1) or 2% (w/v) sucrose (YP-Sucrose; all remaining figures). For growth analysis on solid plates (Fig. 2C), yeast cells were grown in YP-Sucrose before spotting onto YP-Sucrose or YPEG [1% (w/v) yeast extract, 2% (w/v) tryptone, 1% (v/v) ethanol, and 3% (v/v) glycerol] plates [2% (w/v) Bacto agar].

### Antibodies

Mouse monoclonal antibodies against the FLAG (M2; F3165) and HA (HA-7; H9658) tags were from Sigma-Aldrich. Rabbit polyclonal antibodies against the FLAG (SAB4301135) and HA (51064-2-AP) tags were from Sigma-Aldrich and Proteintech, respectively. Other antibodies include the anti-Aac2 monoclonal antibodies 6H8 and 2C10 (65), rabbit anti-Tom70 (66), anti-Atp1/2 (67), anti-Por1 (68), anti-Kgd1 and anti-Cor2 (69), anti-Aac2 (19), anti-Cox1 (70), anti-Cox2 (71), anti-Cox4, anti-Rip1, and anti-Qcr6 (72), anti-Om45 (73), and horseradish peroxidase-conjugated (Figs. 1; 2F; 3B; 4; 5, A and F; and 6, A and E; and figs. S1 and S2) and DyLight fluorophore-conjugated (Figs. 2, B and E; 5, D and E; and 6D) secondary antibodies (Thermo Fisher Scientific).

### In vitro reconstitution of mitochondria with CL

Isolated mitochondria were reconstituted with exogenous CL as described previously (37). Briefly, 400  $\mu$ g of mitochondria from WT or *crd1 $\Delta$*  yeast was resuspended in 40  $\mu$ l of reconstitution buffer [50 mM NaCl and 50 mM imidazole-HCl (pH 7.0)]. CL or PC from a stock solution [20 mg/ml in 5% (w/v) digitonin and 50% (v/v) ethanol] was added to mitochondria in 0.5:10, 1:10, and 1.5:10 lipid:protein (g/g) ratios. The digitonin concentration was adjusted to 0.5 g/g of protein. After 2 hours incubation on ice, samples were solubilized with digitonin. To normalize the different Aac2 extraction efficiencies (fig. S1), the final concentration (w/v) of digitonin was set as follows: to WT, 1.5% for mock and CL pretreated and 2.0% for PC pretreated; to *crd1 $\Delta$* , 1.0% for mock and CL pretreated and 1.5% for PC pretreated. The extracts were resolved on 6 to 16% BN-PAGE gels.

### Limited proteolysis

Isolated WT and *crd1 $\Delta$*  mitochondria (440  $\mu$ g) were incubated with BB7.4 [0.6 M sorbitol and 20 mM Hepes-KOH (pH 7.4)], BB7.4 containing 40  $\mu$ M CATR, or BB6.0 [0.6 M sorbitol and 20 mM MES-KOH (pH 6.0)] containing 10  $\mu$ M BKA for 15 min on ice and then divided into four equal aliquots (100  $\mu$ g). Mitochondrial pellets were collected by sedimentation at 21,000g for 5 min at 4°C and then solubilized with 1.5% (w/v) digitonin lysis buffer [20 mM tris-Cl (pH 7.4), 100 mM NaCl, 20 mM imidazole, 1 mM CaCl<sub>2</sub>, and 10% (v/v) glycerol] spiked with increasing amounts of trypsin (0, 0.5, 5, and 50  $\mu$ g/ml) for 30 min on ice. Trypsin was inactivated by adding 5 $\times$  soybean trypsin inhibitor (5  $\mu$ g), and the clarified extracts were resolved by 10 to 16% SDS-PAGE and immunoblotted as designated.

### Bioinformatics and modeling

Predicted molecular weights of Aac2 C-terminal peptides were performed using the ExPASy Compute pI/Mw tool (74, 75). *S. cerevisiae* Aac2 in the c-state was analyzed using Protein Data Bank (PDB) ID: 4C9G (5). The model of *S. cerevisiae* Aac2 in the m-state was generated with Swiss-Model (76), using the *S. cerevisiae* sequence and the structure of the *Thermus thermophilus* AAC (PDB ID: 6GCI) as a model (10).

### Immunoprecipitation

As indicated, mitochondria (250  $\mu$ g per immunoprecipitation) were incubated with BB7.4 [0.6 M sorbitol and 20 mM Hepes-KOH (pH 7.4)] containing 40  $\mu$ M CATR or BB6.0 [0.6 M sorbitol and 20 mM MES-KOH (pH 6.0)] containing 10  $\mu$ M BKA for 15 min on ice. Mitochondrial pellets were collected by sedimentation at 21,000g for 5 min at 4°C and then solubilized with lysis buffer [20 mM tris-Cl (pH 7.4), 100 mM NaCl, 20 mM imidazole, 1 mM CaCl<sub>2</sub> and 10% (v/v) glycerol] spiked with 1 mM phenylmethylsulfonyl fluoride, 2  $\mu$ M pepstatin A, and 10  $\mu$ M leupeptin and supplemented with either 1.5% (w/v) digitonin or the indicated amount (w/v) of DDM, at a final concentration of 5 mg/ml on ice for 30 min. After centrifugation at 21,000g for 30 min at 4°C, extracts were transferred to 1.5-ml tubes containing FLAG (GenScript) or HA (Sigma-Aldrich) resin and lysis buffer base containing protease inhibitors for a final volume of 1 ml and rotated for 2 hours at 4°C. The contents were then centrifuged at 2000 rpm for 2 min at 4°C and the unbound material collected. Resin was sequentially washed (1 ml and 10 min rotating at 4°C per wash) with lysis buffer base containing 0.1% (w/v) detergent, once with high-salt wash buffer [0.1% (w/v) detergent, 20 mM tris-Cl (pH 7.4), 250 mM NaCl, 20 mM imidazole, 1 mM CaCl<sub>2</sub>, and 10% (v/v) glycerol] and once more with 0.1% (w/v) detergent-containing

lysis buffer base. For the experiments comparing mitochondria with or without mtDNA (Fig. 5F), two additional washes were performed, one with 0.1% (w/v) detergent-containing lysis buffer base and the other with high-salt wash buffer. Resin-bound material was released by boiling in 1× reducing sample buffer and loaded onto custom-made 10 to 16% SDS-PAGE gels.

### Miscellaneous

Isolation of mitochondria, yeast whole-cell extract, steady-state <sup>32</sup>P-based phospholipid analyses, one-dimensional (1D) BN-PAGE, and immunoblotting were performed as previously described (19, 77–79). To determine the effect of Aac inhibitors on Aac2 assembly, mitochondria were preincubated in BB7.4 ± 40 μM CATR or BB6.0 ± 10 μM BKA. After 15 min on ice, mitochondria were pelleted and solubilized with 1.5% (w/v) digitonin or the indicated amount (w/v) of DDM, at a final concentration of 5 mg/ml for 30 min on ice. After a clarifying spin (21,000g for 30 min at 4°C), 10× BN-PAGE sample buffer [5% (w/v) Coomassie brilliant blue G-250 (Serva), 0.5 M 6-aminocaproic acid, and 10 mM bis-tris/HCl (pH 7.0)] was added to the extracts, which were then resolved by 1D BN-PAGE using custom-made 6 to 16% polyacrylamide gradient gels. In the experiments presented in this study, CATR (C4992) and BKA (B6179) were from Sigma-Aldrich. We noted that the ability of BKA to stabilize Aac2 in the absence of CL varied depending on the source of BKA. Ten micromolar of BKA from Enzo Life Sciences (BML-CM113) only weakly stabilized Aac2 in the absence of CL, in contrast to BKA from Sigma-Aldrich. Molecular weight markers used in this study were from Thermo Fisher Scientific (26616 for SDS-PAGE) and GE Healthcare (17044501 for BN-PAGE).

### Statistical analysis

Immunoblots and thin-layer chromatography (TLC) plates for phospholipid studies were quantitated by Quantity One Software (Bio-Rad Laboratories). Statistical analyses were performed using SigmaPlot 11 software (Systat Software, San Jose, CA). All plots show the means ± SEM. The statistical tests performed, sample sizes, and determined *P* values are provided in the figure or its accompanying legend. Representative images (blots and TLCs) from at least three independent experiments performed on at least three separate days are presented in the figures.

### SUPPLEMENTARY MATERIALS

Supplementary material for this article is available at <http://advances.sciencemag.org/cgi/content/full/6/35/eabb0780/DC1>

[View/request a protocol for this paper from Bio-protocol.](#)

### REFERENCES AND NOTES

- M. S. Almen, K. J. Nordstrom, R. Fredriksson, H. B. Schiöth, Mapping the human membrane proteome: A majority of the human membrane proteins can be classified according to function and evolutionary origin. *BMC Biol.* **7**, 50 (2009).
- P. J. Höglund, K. J. V. Nordström, H. B. Schiöth, R. Fredriksson, The solute carrier families have a remarkably long evolutionary history with the majority of the human families present before divergence of bilaterian species. *Mol. Biol. Evol.* **28**, 1531–1541 (2011).
- A. César-Razquin, B. Snijder, T. Frappier-Brinton, R. Isserlin, G. Gyimesi, X. Bai, R. A. Reithmeier, D. Hepworth, M. A. Hediger, A. M. Edwards, G. Superti-Furga, A call for systematic research on solute carriers. *Cell* **162**, 478–487 (2015).
- M. Klingenberg, The ADP and ATP transport in mitochondria and its carrier. *Biochim. Biophys. Acta* **1778**, 1978–2021 (2008).
- J. J. Ruprecht, A. M. Hellawell, M. Harding, P. G. Crichton, A. J. McCoy, E. R. S. Kunji, Structures of yeast mitochondrial ADP/ATP carriers support a domain-based alternating-access transport mechanism. *Proc. Natl. Acad. Sci. U.S.A.* **111**, E426–E434 (2014).
- E. R. S. Kunji, M. Harding, Projection structure of the atractyloside-inhibited mitochondrial ADP/ATP carrier of *Saccharomyces cerevisiae*. *J. Biol. Chem.* **278**, 36985–36988 (2003).
- J. E. Lawson, M. Gawaz, M. Klingenberg, M. G. Douglas, Structure-function studies of adenine nucleotide transport in mitochondria. I. Construction and genetic analysis of yeast mutants encoding the ADP/ATP carrier protein of mitochondria. *J. Biol. Chem.* **265**, 14195–14201 (1990).
- H. Nury, C. Dahout-Gonzalez, V. Trézéguet, G. Lauquin, G. Brandolin, E. Pebay-Peyroula, Structural basis for lipid-mediated interactions between mitochondrial ADP/ATP carrier monomers. *FEBS Lett.* **579**, 6031–6036 (2005).
- E. Pebay-Peyroula, C. Dahout-Gonzalez, R. Kahn, V. Trézéguet, G. J.-M. Lauquin, G. Brandolin, Structure of mitochondrial ADP/ATP carrier in complex with carboxyatractyloside. *Nature* **426**, 39–44 (2003).
- J. J. Ruprecht, M. S. King, T. Zögg, A. A. Aleksandrova, E. Pardon, P. G. Crichton, J. Steyaert, E. R. S. Kunji, The molecular mechanism of transport by the mitochondrial ADP/ATP carrier. *Cell* **176**, 435–447.e15 (2019).
- M. R. Block, G. Zaccari, G. J. Lauquin, P. V. Vignais, Small angle neutron scattering of the mitochondrial ADP/ATP carrier protein in detergent. *Biochem. Biophys. Res. Commun.* **109**, 471–477 (1982).
- M. K. Dienhart, R. A. Stuart, The yeast Aac2 protein exists in physical association with the cytochrome bc1-COX supercomplex and the TIM23 machinery. *Mol. Biol. Cell* **19**, 3934–3943 (2008).
- S. D. Dyal, S. C. Agius, C. De Marcos Lousa, V. Trezeguet, K. Tokatlidis, The dynamic dimerization of the yeast ADP/ATP carrier in the inner mitochondrial membrane is affected by conserved cysteine residues. *J. Biol. Chem.* **278**, 26757–26764 (2003).
- H. Hackenberg, M. Klingenberg, Molecular weight and hydrodynamic parameters of the adenosine 5'-diphosphate-adenosine 5'-triphosphate carrier in Triton X-100. *Biochemistry* **19**, 548–555 (1980).
- L. Bamber, M. Harding, P. J. Butler, E. R. Kunji, Yeast mitochondrial ADP/ATP carriers are monomeric in detergents. *Proc. Natl. Acad. Sci. U.S.A.* **103**, 16224–16229 (2006).
- L. Bamber, M. Harding, M. Monne, D. J. Slotboom, E. R. Kunji, The yeast mitochondrial ADP/ATP carrier functions as a monomer in mitochondrial membranes. *Proc. Natl. Acad. Sci. U.S.A.* **104**, 10830–10834 (2007).
- L. Bamber, D. J. Slotboom, E. R. Kunji, Yeast mitochondrial ADP/ATP carriers are monomeric in detergents as demonstrated by differential affinity purification. *J. Mol. Biol.* **371**, 388–395 (2007).
- P. G. Crichton, M. Harding, J. J. Ruprecht, Y. Lee, E. R. Kunji, Lipid, detergent, and Coomassie Blue G-250 affect the migration of small membrane proteins in blue native gels: mitochondrial carriers migrate as monomers not dimers. *J. Biol. Chem.* **288**, 22163–22173 (2013).
- S. M. Claypool, Y. Oktay, P. Boonthueung, J. A. Loo, C. M. Koehler, Cardiolipin defines the interactome of the major ADP/ATP carrier protein of the mitochondrial inner membrane. *J. Cell Biol.* **182**, 937–950 (2008).
- Y.-W. Lu, M. G. Acoba, K. Selvaraju, T.-C. Huang, R. S. Nirujogi, G. Sathe, A. Pandey, S. M. Claypool, Human adenine nucleotide translocases physically and functionally interact with respirasomes. *Mol. Biol. Cell* **28**, 1489–1506 (2017).
- C. S. Mehnert, H. Rampelt, M. Gebert, S. Oeljeklaus, S. G. Schrempp, L. Kochbeck, B. Guiard, B. Warscheid, M. van der Laan, The mitochondrial ADP/ATP carrier associates with the inner membrane presequence translocase in a stoichiometric manner. *J. Biol. Chem.* **289**, 27352–27362 (2014).
- H. Schagger, K. Pfeiffer, Supercomplexes in the respiratory chains of yeast and mammalian mitochondria. *EMBO J.* **19**, 1777–1783 (2000).
- M. G. Baile, Y.-W. Lu, S. M. Claypool, The topology and regulation of cardiolipin biosynthesis and remodeling in yeast. *Chem. Phys. Lipids* **179**, 25–31 (2014).
- Y. W. Lu, S. M. Claypool, Disorders of phospholipid metabolism: an emerging class of mitochondrial disease due to defects in nuclear genes. *Front. Genet.* **6**, 3 (2015).
- K. Beyer, M. Klingenberg, ADP/ATP carrier protein from beef heart mitochondria has high amounts of tightly bound cardiolipin, as revealed by 31P nuclear magnetic resonance. *Biochemistry* **24**, 3821–3826 (1985).
- K. Beyer, B. Nuscher, Specific cardiolipin binding interferes with labeling of sulfhydryl residues in the adenosine diphosphate/adenosine triphosphate carrier protein from beef heart mitochondria. *Biochemistry* **35**, 15784–15790 (1996).
- K. S. Eble, W. B. Coleman, R. R. Hantgan, C. C. Cunningham, Tightly associated cardiolipin in the bovine heart mitochondrial ATP synthase as analyzed by 31P nuclear magnetic resonance spectroscopy. *J. Biol. Chem.* **265**, 19434–19440 (1990).
- G. Fiermonte, V. Dolce, F. Palmieri, Expression in *Escherichia coli*, functional characterization, and tissue distribution of isoforms A and B of the phosphate carrier from bovine mitochondria. *J. Biol. Chem.* **273**, 22782–22787 (1998).
- M. Fry, D. Green, Cardiolipin requirement for electron transfer in complex I and III of the mitochondrial respiratory chain. *J. Biol. Chem.* **256**, 1874–1880 (1981).
- B. Gomez Jr., N. C. Robinson, Quantitative determination of cardiolipin in mitochondrial electron transferring complexes by silicic acid high-performance liquid chromatography. *Anal. Biochem.* **267**, 212–216 (1999).



31. B. Gomez Jr., N. C. Robinson, Phospholipase digestion of bound cardiolipin reversibly inactivates bovine cytochrome bc1. *Biochemistry* **38**, 9031–9038 (1999).
32. B. Kadenbach, P. Mende, H. V. Kolbe, I. Stipani, F. Palmieri, The mitochondrial phosphate carrier has an essential requirement for cardiolipin. *FEBS Lett.* **139**, 109–112 (1982).
33. C. Lange, J. H. Nett, B. L. Trumpower, C. Hunte, Specific roles of protein-phospholipid interactions in the yeast cytochrome bc1 complex structure. *EMBO J.* **20**, 6591–6600 (2001).
34. E. Sedlak, N. C. Robinson, Phospholipase A(2) digestion of cardiolipin bound to bovine cytochrome c oxidase alters both activity and quaternary structure. *Biochemistry* **38**, 14966–14972 (1999).
35. K. Shinzawa-Itoh, H. Aoyama, K. Muramoto, H. Terada, T. Kurauchi, Y. Tadehara, A. Yamasaki, T. Sugimura, S. Kurono, K. Tsujimoto, T. Mizushima, E. Yamashita, T. Tsukihara, S. Yoshikawa, Structures and physiological roles of 13 integral lipids of bovine heart cytochrome c oxidase. *EMBO J.* **26**, 1713–1725 (2007).
36. S. B. Vik, G. Georgevich, R. A. Capaldi, Diphosphatidylglycerol is required for optimal activity of beef heart cytochrome c oxidase. *Proc. Natl. Acad. Sci. U.S.A.* **78**, 1456–1460 (1981).
37. K. Pfeiffer, V. Gohil, R. A. Stuart, C. Hunte, U. Brandt, M. L. Greenberg, H. Schägger, Cardiolipin stabilizes respiratory chain supercomplexes. *J. Biol. Chem.* **278**, 52873–52880 (2003).
38. J. Zhang, Z. Guan, A. N. Murphy, S. E. Wiley, G. A. Perkins, C. A. Worby, J. L. Engel, P. Heacock, O. K. Nguyen, J. H. Wang, C. R. H. Raetz, W. Dowhan, J. E. Dixon, Mitochondrial phosphatase PTPMT1 is essential for cardiolipin biosynthesis. *Cell Metab.* **13**, 690–700 (2011).
39. M. Zhang, E. Mileykovskaya, W. Dowhan, Gluing the respiratory chain together. Cardiolipin is required for supercomplex formation in the inner mitochondrial membrane. *J. Biol. Chem.* **277**, 43553–43556 (2002).
40. G. Hedger, S. L. Rouse, J. Domański, M. Chavent, H. Koldsø, M. S. P. Sansom, Lipid-loving ANTs: Molecular simulations of cardiolipin interactions and the organization of the adenine nucleotide translocase in model mitochondrial membranes. *Biochemistry* **55**, 6238–6249 (2016).
41. F. Jiang, M. T. Ryan, M. Schlame, M. Zhao, Z. Gu, M. Klingenberg, N. Pfanner, M. L. Greenberg, Absence of cardiolipin in the *crd1* null mutant results in decreased mitochondrial membrane potential and reduced mitochondrial function. *J. Biol. Chem.* **275**, 22387–22394 (2000).
42. O. B. Ogunbona, M. G. Baile, S. M. Claypool, Cardiomyopathy-associated mutation in the ADP/ATP carrier reveals translation-dependent regulation of cytochrome c oxidase activity. *Mol. Biol. Cell* **29**, 1449–1464 (2018).
43. M. G. Baile, M. Sathappa, Y.-W. Lu, E. Pryce, K. Whited, J. M. McCaffery, X. Han, N. N. Alder, S. M. Claypool, Unremodeled and remodeled cardiolipin are functionally indistinguishable in yeast. *J. Biol. Chem.* **289**, 1768–1778 (2014).
44. V. Koshkin, M. L. Greenberg, Oxidative phosphorylation in cardiolipin-lacking yeast mitochondria. *Biochem. J.* **347** (Pt 3), 687–691 (2000).
45. V. Koshkin, M. L. Greenberg, Cardiolipin prevents rate-dependent uncoupling and provides osmotic stability in yeast mitochondria. *Biochem. J.* **364**, 317–322 (2002).
46. K. Malhotra, A. Modak, S. Nangia, T. H. Daman, U. Gunsell, V. L. Robinson, D. Mokranjac, E. R. May, N. N. Alder, Cardiolipin mediates membrane and channel interactions of the mitochondrial TIM23 protein import complex receptor Tim50. *Sci. Adv.* **3**, e1700532 (2017).
47. P. Singh, Budding Yeast: An Ideal Backdrop for In vivo Lipid Biochemistry. *Front. Cell Dev. Biol.* **4**, 156 (2016).
48. P. G. Crichton, Y. Lee, J. J. Ruprecht, E. Cerson, C. Thangaratnarajah, M. S. King, E. R. S. Kunji, Trends in thermostability provide information on the nature of substrate, inhibitor, and lipid interactions with mitochondrial carriers. *J. Biol. Chem.* **290**, 8206–8217 (2015).
49. M. Klingenberg, M. Appel, W. Babel, H. Aquila, The binding of bongkrekate to mitochondria. *Eur. J. Biochem.* **131**, 647–654 (1983).
50. S. Luciani, R. Varotto, Difference between atractyloside and carboxyatractyloside on the binding to the mitochondrial membrane. *FEBS Lett.* **56**, 194–197 (1975).
51. O. B. Ogunbona, O. Onguka, E. Calzada, S. M. Claypool, Multitiered and cooperative surveillance of mitochondrial phosphatidylserine decarboxylase 1. *Mol. Cell. Biol.* **37**, e00049-17 (2017).
52. V. M. Gohil, P. Hayes, S. Matsuyama, H. Schägger, M. Schlame, M. L. Greenberg, V. M. Gohil, P. Hayes, S. Matsuyama, H. Schägger, M. Schlame, M. L. Greenberg, Cardiolipin biosynthesis and mitochondrial respiratory chain function are interdependent. *J. Biol. Chem.* **279**, 42612–42618 (2004).
53. L. Böttinger, C. U. Mårtensson, J. Song, N. Zufall, N. Wiedemann, T. Becker, Respiratory chain supercomplexes associate with the cysteine desulfurase complex of the iron-sulfur cluster assembly machinery. *Mol. Biol. Cell* **29**, 776–785 (2018).
54. M. S. King, M. Kerr, P. G. Crichton, R. Springett, E. R. S. Kunji, Formation of a cytoplasmic salt bridge network in the matrix state is a fundamental step in the transport mechanism of the mitochondrial ADP/ATP carrier. *Biochim. Biophys. Acta* **1857**, 14–22 (2016).
55. R. Kramer, M. Klingenberg, Modulation of the reconstituted adenine nucleotide exchange by membrane potential. *Biochemistry* **19**, 556–560 (1980).
56. J. S. Sousa, D. J. Mills, J. Vonck, W. Kuhlbrandt, Functional asymmetry and electron flow in the bovine respirasome. *eLife* **5**, e21290 (2016).
57. J. Gu, M. Wu, R. Guo, K. Yan, J. Lei, N. Gao, M. Yang, The architecture of the mammalian respirasome. *Nature* **537**, 639–643 (2016).
58. J. A. Letts, K. Fiedorczuk, L. A. Sazanov, The architecture of respiratory supercomplexes. *Nature* **537**, 644–648 (2016).
59. M. Wu, J. Gu, R. Guo, Y. Huang, M. Yang, Structure of mammalian respiratory supercomplex I<sub>1</sub>III<sub>2</sub>IV<sub>1</sub>. *Cell* **167**, 1598–1609.e10 (2016).
60. D. Milenkovic, J. N. Blaza, N.-G. Larsson, J. Hirst, The enigma of the respiratory chain supercomplex. *Cell Metab.* **25**, 765–776 (2017).
61. A. J. Chicco, G. C. Sparagna, Role of cardiolipin alterations in mitochondrial dysfunction and disease. *Am. J. Physiol. Cell Physiol.* **292**, C33–C44 (2007).
62. S. M. Claypool, C. M. Koehler, The complexity of cardiolipin in health and disease. *Trends Biochem. Sci.* **37**, 32–41 (2012).
63. A. Wach, A. Brachat, R. Pohlmann, P. Philippsen, New heterologous modules for classical or PCR-based gene disruptions in *Saccharomyces cerevisiae*. *Yeast* **10**, 1793–1808 (1994).
64. E. S. Goldring, L. I. Grossman, D. Krupnick, D. R. Cryer, J. Marmur, The petite mutation in yeast. Loss of mitochondrial deoxyribonucleic acid during induction of petites with ethidium bromide. *J. Mol. Biol.* **52**, 323–335 (1970).
65. V. Panneels, U. Schussler, S. Costagliola, I. Sinning, Choline head groups stabilize the matrix loop regions of the ATP/ADP carrier ScaAC2. *Biochem. Biophys. Res. Commun.* **300**, 65–74 (2003).
66. H. Riezman, R. Hay, S. Gasser, G. Daum, G. Schneider, C. Witte, G. Schatz, The outer membrane of yeast mitochondria: Isolation of outside-out sealed vesicles. *EMBO J.* **2**, 1105–1111 (1983).
67. M. L. Maccacchini, Y. Rudin, G. Blobel, G. Schatz, Import of proteins into mitochondria: precursor forms of the extramitochondrially made F1-ATPase subunits in yeast. *Proc. Natl. Acad. Sci. U.S.A.* **76**, 343–347 (1979).
68. G. Daum, P. C. Bohni, G. Schatz, Import of proteins into mitochondria. Cytochrome b2 and cytochrome c peroxidase are located in the intermembrane space of yeast mitochondria. *J. Biol. Chem.* **257**, 13028–13033 (1982).
69. B. S. Glick, A. Brandt, K. Cunningham, S. Miiller, R. L. Hallberg, G. Schatz, Cytochromes c1 and b2 are sorted to the intermembrane space of yeast mitochondria by a stop-transfer mechanism. *Cell* **69**, 809–822 (1992).
70. W. Dowhan, C. R. Bibus, G. Schatz, The cytoplasmically-made subunit IV is necessary for assembly of cytochrome c oxidase in yeast. *EMBO J.* **4**, 179–184 (1985).
71. R. O. Poyton, G. Schatz, Cytochrome c oxidase from bakers' yeast. III. Physical characterization of isolated subunits and chemical evidence for two different classes of polypeptides. *J. Biol. Chem.* **250**, 752–761 (1975).
72. M. G. Baile, K. Whited, S. M. Claypool, Deacylation on the matrix side of the mitochondrial inner membrane regulates cardiolipin remodeling. *Mol. Biol. Cell* **24**, 2008–2020 (2013).
73. M. Ohba, G. Schatz, Protein import into yeast mitochondria is inhibited by antibodies raised against 45-kd proteins of the outer membrane. *EMBO J.* **6**, 2109–2115 (1987).
74. B. Bjellqvist, G. J. Hughes, C. Pasquali, N. Paquet, F. Ravier, J.-C. Sanchez, S. Frutiger, D. Hochstrasser, The focusing positions of polypeptides in immobilized pH gradients can be predicted from their amino acid sequences. *Electrophoresis* **14**, 1023–1031 (1993).
75. H. C. Gasteiger, E. Gattiker, A. Duvaud, S. Wilkins, M. R., Appel, R. D., Bairoch, A., Protein Identification and Analysis Tools on the ExPASy Server, in *The Proteomics Protocols Handbook*, J. M. Walker, Ed. (Humana Press, 2005), pp. 571–607.
76. A. Waterhouse, M. Bertoni, S. Bienert, G. Studer, G. Tauriello, R. Gumienny, F. T. Heer, T. A. P. de Beer, C. Rempfer, L. Bordoli, R. Lepore, T. Schwede, SWISS-MODEL: Homology modelling of protein structures and complexes. *Nucleic Acids Res.* **46**, W296–W303 (2018).
77. E. Calzada, E. Avery, P. N. Sam, A. Modak, C. Wang, J. M. McCaffery, X. Han, N. N. Alder, S. M. Claypool, Phosphatidylethanolamine made in the inner mitochondrial membrane is essential for yeast cytochrome bc1 complex function. *Nat. Commun.* **10**, 1432 (2019).
78. S. M. Claypool, J. M. McCaffery, C. M. Koehler, Mitochondrial mislocalization and altered assembly of a cluster of Barth syndrome mutant tafazzins. *J. Cell Biol.* **174**, 379–390 (2006).
79. O. Onguka, E. Calzada, O. B. Ogunbona, S. M. Claypool, Phosphatidylserine decarboxylase 1 autocatalysis and function does not require a mitochondrial-specific factor. *J. Biol. Chem.* **290**, 12744–12752 (2015).

**Acknowledgments:** We would like to thank C. Koehler (UCLA) for many of the antibodies used in this study. **Funding:** This work was supported by grants from the NIH (R01HL108882 to S.M.C. and Biochemistry, Cellular, and Molecular Biology Program Training grant T32GM007445 to M.G.B. and Y.L.), predoctoral fellowships from the American Heart Association (15PRE24480066 to O.B.O., 10PRE3280013 to M.G.B., and

12PRE11910004 to Y.L.), and a postdoctoral fellowship from the Uehara Memorial Foundation (to N.S.). **Author contributions:** N.S., S.K., and S.M.C. performed experiments and co-wrote the manuscript. O.B.O., M.G.B., and Y.L. performed experiments and edited the manuscript. **Competing interests:** The authors declare that they have no competing interests. **Data and materials availability:** All data supporting the findings of this study are available within the paper and the Supplementary Materials. Additional data related to this paper may be requested from the authors. Correspondence and material requests should be directed to S.M.C.

Submitted 28 January 2020  
Accepted 8 July 2020  
Published 28 August 2020  
10.1126/sciadv.abb0780

**Citation:** N. Senoo, S. Kandasamy, O. B. Ogunbona, M. G. Baile, Y. Lu, S. M. Claypool, Cardiolipin, conformation, and respiratory complex-dependent oligomerization of the major mitochondrial ADP/ATP carrier in yeast. *Sci. Adv.* **6**, eabb0780 (2020).